

Effect, Ergänzungsband, 1931-1937 (Springer, Berlin, 1938). From Table I one readily finds that the combinations of vibrational levels which add to the methyl (ν_{11}) 2928-cm⁻¹ frequency within a bandwidth of ~ 100 cm⁻¹ (besides the previously mentioned processes $2\nu_8 = 2910$ cm⁻¹, $2\nu_1^* = 2968$ cm⁻¹, and $\nu_1^* + \nu_8 = 2939$ cm⁻¹) are the three-quantum processes $\nu_8 + \nu_5 + \nu_2 = 2938$ cm⁻¹, and $\nu_7 + 2\nu_3 = 2902$ cm⁻¹, where ν_8 is the CH₃ internal vibration, ν_1^* , ν_5 , and ν_3 are the hydrogen angle variation modes, ν_2 is C-C-O skeleton vibration, and ν_7 is a CH₂ internal vibrational mode. Therefore, besides the ν_8 and ν_1^* levels, the 2928-cm⁻¹ mode might also decay to the vibrational levels ν_2 , ν_3 , ν_5 , and ν_7 . However, the latter four levels are reached via three-quantum processes which are usually less probable than two-quantum processes of the type $2\nu_8$, $2\nu_1^*$, and $\nu_1^* + \nu_8$, and are therefore more difficult to detect.

⁸Recently, the dephasing time and depopulation times have been measured using picosecond probe Raman techniques (Ref. 3). When the probe beam is applied at an angle of incidence such that the probe beam, probe Raman intensity, and vibration (created via SRS from the exciting laser) are phase matched together, the measured lifetime is the dephasing time since the probe Raman scattering intensity is sensitive to both the phase and population changes of the molecular vibrations. However, when the probe Raman scattering is detected in a direction in which the phase matching to the created molecular vibration is unimportant, the measured decay time is the depopulation time since the probe Raman intensity is only sensitive to population changes of the molecular vibrations. It has been found (Ref. 3) that $\tau(\text{depopulation}) > \tau(\text{dephasing})$.

⁹The lifetimes of the 2928- and 1454-cm⁻¹ vibrations are $\tau_0 \sim 28$ psec and τ_1 , respectively. To estimate whether the difference-frequency term is operative, the anti-Stokes Raman signal at 1454 cm⁻¹ is defined to be proportional to $\beta_1 n_1(t) + \beta_2 n_2(t)$, and the anti-Stokes Raman signal at 2928 cm⁻¹ is defined to be proportional to $\beta_0 n_2(t)$, where $n_2(t)$ and $n_1(t)$ are the populations of the 2928- and 1454-cm⁻¹ levels, respectively, and the β coefficients denote the spontaneous Raman scattering efficiencies. The term $\beta_1 n_1(t)$ is the contribution due to direct scattering from the 1454-cm⁻¹ vibrational level, the term $\beta_2 n_2(t)$ arises as a result of scattering involving the difference frequency between the 2928- and 1454-cm⁻¹ levels, and the term $\beta_0 n_2(t)$ represents the direct scattering off the 2928-cm⁻¹ vibrational level. From spontaneous Raman scattering data (Ref. 7), the value of β_0 is approximately $2\beta_1$. The value of β_2 in terms of the other β coefficients is not known but can be estimated from the knowledge that the Raman intensity for the combination or difference-frequency process is ~ 0.01 to 1 times the one vibrational quantum process (Ref. 7), and hence $\beta_2 \leq \beta_2$. Taking $\beta_1 = \beta_2$ and $\tau_1 \sim \tau_0/2$, one calculates a delay time of ~ 8 psec between the peaks of the 2928- and 1454-cm⁻¹ anti-Stokes shifted signals and a peak anti-Stokes Raman intensity ratio $I(1454)/I(2928)$ of $\sim \frac{1}{2}$; taking $\beta_1 = \beta_2$ and $\tau_1 \sim \tau_0$, one finds a time of 14 psec between the peak signals and an anti-Stokes Raman intensity ratio of ~ 0.7 . If β_1 is chosen to be substantially greater than β_2 , the calculated Raman intensity ratio does not agree with the experimentally observed value—therefore the suspicion that the difference-frequency process may be playing a role.

Interpretation of an Enhanced Diffusion Observed in a Solid-State Plasma*

H. Okuda, J. M. Dawson, and W. M. Hooke

Plasma Physics Laboratory, Princeton University, Princeton, New Jersey 08540

(Received 7 August 1972)

An enhanced Bohm-like diffusion across a magnetic field observed in a germanium plasma near thermal equilibrium can be interpreted in terms of vortex diffusion due to plasma convections which are thermally excited. Both theoretical analysis and numerical simulation show good agreement with the experimental observations.

In this note we show by numerical simulation that an enhanced Bohm-like diffusion observed in a germanium plasma by Gurnee, Hooke, Goldsmith, and Brennan¹ can be interpreted in terms of vortex diffusion due to plasma convective cells.²⁻⁴ These authors found that, for $\omega_{ce}\tau_n > 3.5$ (where ω_{ce} is the electron gyrofrequency, and τ_n is the electron scattering time with the lattice), the diffusion across a magnetic field is more rapid than predicted by collision theory which takes

into account the scattering of particles with the lattice.¹ The observed enhanced diffusion follows more or less a Bohm-like law, $D_{\perp} \propto 1/B$. They confirmed that the enhanced diffusion is reproducible, and they could not detect any enhanced fluctuations though enhanced fluctuations of a few times the thermal level would not be detectable.

We show by numerical simulation in three dimensions that a similar enhanced plasma diffusion can be reproduced for the same parameters

found in the real experiment. A theoretical analysis will also be given to explain the observed enhanced diffusion. The enhanced diffusion can be interpreted in terms of plasma convective cells.²⁻⁴

The mass ratio of the electrons to the ions (holes) in a germanium plasma is close to unity and furthermore, the number of particles in a Debye length is a small number. It is feasible to simulate such a plasma using the techniques developed recently for plasma computer simulations.⁵ Rapid collisions of particles with the lattice may be included in the model by using a Monte Carlo method to scatter the particles randomly at a given scattering rate. The effect of the dielectric properties of germanium is also taken into account.⁶ In the numerical experiments the finite size of the particles gives some modification, especially at the highest field B where the Larmor orbits are becoming smaller than a particle size.

The computer model used was a three-dimensional electrostatic particle model with a uniform magnetic field in the z direction.⁷ The simulation is carried out in a cube with a $32 \times 32 \times 32$ spatial grid. Both ions and electrons have Maxwell velocity distributions with the same temper-

ature. The cross-field diffusion coefficient is measured by following the guiding-center displacement in time of a set of test ions and electrons $\{D_{\perp} = [(\Delta x_g)^2 + (\Delta y_g)^2]t\}$.

Figure 1(a) shows results of simulations with the two different collision times of $\omega_p \tau_n = 10$ and 1. Note that the plasma is quite collisional and, therefore, it is not important whether or not the field lines are closed, in contrast to what was found earlier for collisionless plasmas.^{3,4} The parameters of the simulations are taken from the real experiment: $n\lambda_D^3 \approx 3.5$, $m_e/m_i = 1.5$, and the magnetic field was changed so that ω_{pe}/ω_{ce} varied from 2 to $\frac{1}{32}$. Note that the simulation shows classical behavior ($D_{\perp} \propto 1/B^2$) for weak fields and anomalous Bohm-like behavior ($D_{\perp} \propto 1/B$) for stronger fields for both cases. The Coulomb collision time is much larger than the collision time with the lattice and, therefore, the observed value of the diffusion is about 1 order of magnitude greater than that due to "Coulomb scattering." However, the small Coulomb field becomes important for high magnetic fields, since it causes the enhanced diffusion through collective $c\vec{E} \times \vec{B}/B^2$ drift.

The physical mechanism for the enhanced diffu-

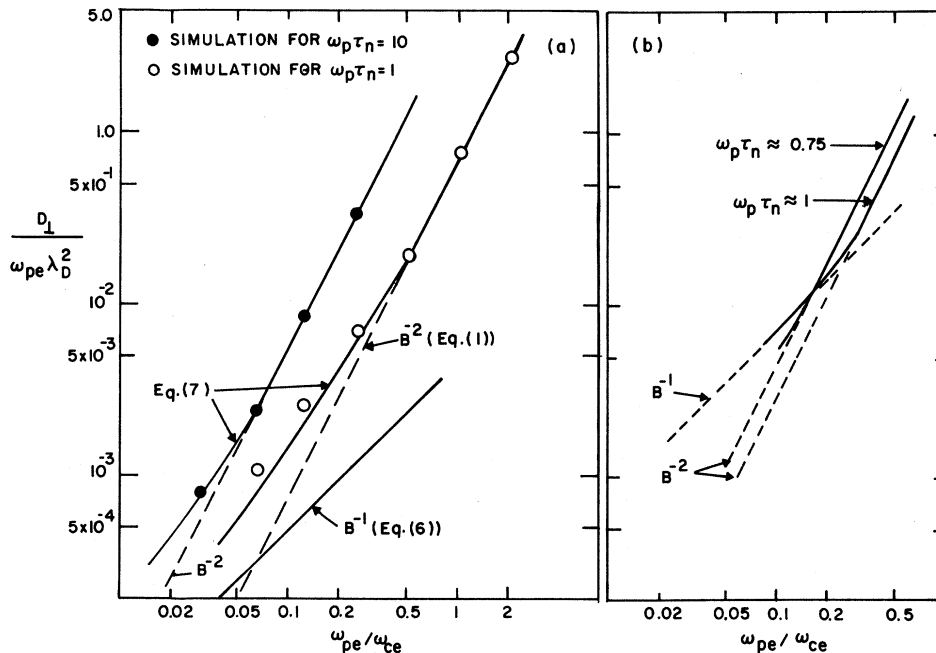


FIG. 1. (a) Two sets of simulation experiments with collision times of $\omega_p \tau_n = 10$ and 1. Note that for both cases, the diffusion is enhanced above the classical value and takes Bohm-type behavior for strong fields. $\lambda_D = 4$, $n\lambda_D^3 = 3.5$, $m_e/m_i = 1.5$, and a $32 \times 32 \times 32$ grid were used. (b) Two results from the solid-state experiments with $\omega_p \tau_n \approx 1$ ($T = 92^\circ\text{K}$) and 0.75 ($T = 111^\circ\text{K}$). Note that the classical diffusion is followed by the Bohm-like diffusion for high fields.

sion may be interpreted as being due to thermally excited convective cells which were studied earlier in detail.²⁻⁴ When the collision rate is low ($\omega_p\tau_n=10$), then the convective flow carries the plasma across the field for modest values of B_0 . For a very high collision rate ($\omega_p\tau_n=1$), the convective motion is damped by the rapid collisions. However, when the magnetic field is high enough so that $\omega_c\tau_n \gg 1$, then even here there is an appreciable plasma flow across fields. This occurs when the gyroradius of plasma particles becomes smaller than the convective cells.

Two typical results from the solid-state experiments with different temperatures¹ are shown in Fig. 1(b), for comparison. They correspond to the cases of $\omega_p\tau_n \approx 1$ and 0.75. The first experiment shows classical behavior ($D_\perp \propto 1/B^2$) for weak fields and anomalous behavior ($D_\perp \propto 1/B$) for stronger fields; the second experiment shows classical diffusion over essentially the whole range of B although there is an indication of a deviation at the largest value of B . The B^{-2} diffusion agrees with the theory which takes into account the scattering with the lattice but neglects the self-consistent convective motion.¹ We have compared the absolute value of diffusion with that in the simulation as well as the break point from the collisional to convective diffusion regions. The resemblance of the experiment and the simulation is striking; the break points between the classical behavior and the enhanced diffusion agree reasonably well with each other, although it appears that it occurs somewhat sooner for the solid-state experiment than for the simulation experiment. There may be a number of reasons for the differences; among them are the following: (1) The simulation plasma is rather small and only very small convective motions are allowed in it compared to the experimental plasma. (2) The experimental plasma might have slightly enhanced convective motions (a few times thermal) which are not detected. (3) The solid-state plasma was more complicated than the simulation plasma, containing more than one species of electron and hole. (4) The Monte Carlo method may not have represented collisions with the lattice completely accurately. (5) The experimental plasma has a density gradient not present in the computer plasma. (6) The finite size of the simulation particles will cause some reduction of the convective diffusion.

To estimate the break point, we note that the collisional diffusion coefficient may be written as

$$D_{\text{col}} = \alpha r_L^2 / \tau_n, \quad (1)$$

where α is a numerical coefficient of order unity, and r_L is the gyroradius; α may be determined from Fig. 1. This gives $\alpha \approx 3$ (theory predicts $2\sqrt{2}$) for $\omega_p\tau_n=1$. The convective diffusion is given by

$$D_{\text{con}} = \sum_k \langle v_{k\perp}^2 \rangle \tau_k = \sum_k \langle E_{k\perp}^2 \rangle c^2 / B^2 \tau_k, \quad (2)$$

where $\langle v_{k\perp}^2 \rangle$ and $\langle E_{k\perp}^2 \rangle$ are the average square of convective velocity and the electric field perpendicular to B for the k th mode, and τ_k is its lifetime (decay time or correlation time). From our previous work^{3,4} we know that $\langle E_k^2 \rangle$ is given by

$$\frac{\epsilon \langle E_k^2 \rangle}{8\pi} = \frac{KT}{2L^3(1+k^2\lambda_D^2)(1+4\pi\rho c^2/B^2)}, \quad (3)$$

where ϵ is the dielectric constant of the lattice, ρ is the total plasma density, λ_D is the Debye length, and L^3 is the volume of the plasma. The lifetime for a convective mode may be obtained from fluid equations with collisions with the lattice. They are

$$\begin{aligned} \partial n_{i,e} / \partial t + \nabla \cdot n_{i,e} \vec{v}_{i,e} &= 0, \\ \left(\frac{\partial}{\partial t} + \vec{v}_{i,e} \cdot \nabla \right) \vec{v}_{i,e} &= \frac{\pm e}{m_{i,e}} \left(\vec{E} + \frac{1}{c} \vec{v}_{i,e} \times B_0 \right) \\ &\quad - \frac{KT \nabla n_{i,e}}{m_{i,e} n_{i,e}} - \frac{\vec{v}_{i,e}}{\tau_n}, \\ \nabla \cdot \epsilon \vec{E} &= 4\pi e (n_i - n_e), \\ \vec{E} &= -\nabla \phi. \end{aligned} \quad (4)$$

Linearizing Eqs. (4), we find the lifetime for a convective mode will be

$$\begin{aligned} \frac{1}{\tau_k} &= \left(v_i^2 + \frac{2\omega_p^2}{k^2} \right) k_{\parallel}^2 \tau_n \\ &\quad + \left(\frac{k_{\perp}^2 v_i^2}{\omega_c^2} + \frac{2k_{\perp}^2 \omega_p^2}{k^2 \omega_c^2} \right) \frac{1}{\tau_n}, \end{aligned} \quad (5)$$

where we assumed $m_i \approx m_e$ for a germanium plasma. The first term is the damping rate due to diffusion of particles parallel to B , while the second term is that due to damping of the convective motion due to collisions with the lattice. Substituting $\langle E_k^2 \rangle$ and τ_k into Eq. (2), and assuming that the important modes have wavelengths parallel to B which are larger than those perpendicular to B , we find for $\omega_c/\omega_p > 1$,

$$D_{\text{con}} = \frac{1}{8} (\omega_p/\omega_c) (\omega_p/n\lambda_D). \quad (6)$$

We note that the convective diffusion is independent of the collision rate and gives a Bohm-like diffusion ($D_\perp \propto B^{-1}$) which is consistent with both the simulation and the experiment for large B .

In the transition region of diffusion where collisional and convective diffusions are comparable, the total diffusion will be the sum of two different types of diffusions. Thus, we have

$$D_{\text{tot}} = (\alpha r_L^2 / \tau_n) + \frac{1}{8} (\omega_p / \omega_c) (\omega_p / n \lambda_D), \quad (7)$$

which agrees well with the simulation results as shown in Fig. 1(a). The break points from classical to convective diffusion are also predicted correctly. They are given by

$$\omega_p / \omega_c = \omega_p \tau_n / 8 n \lambda_D^3 \alpha.$$

Finally, we should like to point out that the convective diffusion may also explain measurements of Moore and Kessler⁸ on the magnetic moment of a germanium plasma diffusing across a magnetic field. They found that for $\omega_c \tau_n \lesssim 3$ the measured magnetic moment agrees well with the theory based on the ambipolar diffusion which gives

$$M = -2en\omega_c \tau_n D_a, \quad (8)$$

where

$$D_a = v_t^2 \tau_n / (1 + \omega_c^2 \tau_n^2). \quad (9)$$

However, for $\omega_c \tau_n > 3$, the observation deviates from Eq. (8), which predicts $M \sim 1/B$, and is more or less independent of B .

As we have already pointed out, the convective plasma transport is more important than the collisional transport for $\omega_c / \tau_n \gtrsim 3$ and D should vary as $1/B$ there, which would explain the observed fact that the magnetic moment is independent of B .

In closing, it would be interesting to observe

the three different regions of plasma diffusion²⁻⁴ for a finite-length solid-state plasma. This may be possible if $n \lambda_D^3$ is larger than, say, 100 and the electron lattice collision rate is small enough.

*Work supported jointly by the U. S. Atomic Energy Commission under Contract No. AT (11-1)-3073, and the U. S. Air Force Office of Scientific Research under Contract No. F44620-70-C-0033. Use was made of computer facilities supported in part by National Science Foundation Grant No. NSF-GP 579.

¹M. N. Gurnee, W. M. Hooke, G. J. Goldsmith, and M. H. Brennan, *Phys. Rev. A* **5**, 158 (1972).

²J. M. Dawson, H. Okuda, and R. N. Carlile, *Phys. Rev. Lett.* **27**, 491 (1971).

³H. Okuda and J. M. Dawson, to be published.

⁴H. Okuda and J. M. Dawson, *Phys. Rev. Lett.* **28**, 1625 (1972).

⁵*Methods in Computational Physics*, edited by B. Alder, S. Fernbach, and M. Rotenberg (Academic, New York, 1970), Vol. 9.

⁶The equation of motion of a particle in a dielectric may be written as

$$m_i \frac{d\vec{v}_i}{dt} = \sum_{j \neq i} \frac{q_i q_j (\vec{r}_i - \vec{r}_j)}{\epsilon |\vec{r}_i - \vec{r}_j|^3} + \frac{q_i}{c} \vec{v}_i \times \vec{B},$$

where ϵ is the dielectric constant of the medium.

Therefore, the plasma frequency and the Debye length in a dielectric will be $\omega_p \equiv (4\pi n q^2 / \epsilon m)^{1/2}$ and $\lambda_D^{-2} = \sum_j 4\pi n q_j^2 / \epsilon k T_j$, which are used throughout the paper.

⁷J. M. Dawson, C. G. Hsi, and R. Shanny, *Bull. Amer. Phys. Soc.* **13**, 1744 (1968).

⁸A. R. Moore and J. O. Kessler, *Phys. Rev.* **132**, 1494 (1963).

Dynamical Behavior of He³-He⁴ Mixtures near the Tricritical Point

Kyozi Kawasaki* and James D. Gunton*

Temple University, Philadelphia, Pennsylvania 19122

(Received 16 October 1972)

The dynamical behavior of the normal fluid phase of liquid He³-He⁴ mixtures near the tricritical point is studied. The superfluid order parameter and the entropy fluctuation are shown to have a common characteristic frequency which is the same as that predicted by dynamical scaling for the characteristic frequency of second sound in the ordered phase. The concentration fluctuation is shown to have a smaller characteristic frequency. The critical anomalies of the transport coefficients also are determined.

The unusual thermodynamic properties manifest near tricritical points have recently been the subject of several experimental and theoretical investigations.¹ Here we report on the first theoretical study of the dynamical behavior near tricritical points, concerning ourselves in particular with the liquid He³-He⁴ mixtures in the normal fluid phase. We adopt the notation recently proposed by Griffiths¹